

Microstructure and mechanical properties of Mg–Gd–Zr alloys with low gadolinium contents

Yao-Bo Hu · Juan Deng · Chong Zhao ·
Fu-Sheng Pan · Jian Peng

Received: 16 December 2010 / Accepted: 5 April 2011 / Published online: 12 April 2011
© Springer Science+Business Media, LLC 2011

Abstract Mg– x Gd–0.6Zr ($x = 2, 4$, and 6% mass fraction) alloys were synthesized by semi-continuous casting process. The effects of gadolinium content and aging time on microstructures and mechanical properties of the Mg– x Gd–0.6Zr alloys were investigated. The results show that the microstructures of the as-cast GKx ($x = 2, 4$, and 6%) alloys are typical grain structures and no Gd dendritic segregation. In as-cast Mg–6Gd–0.6Zr alloy, the second phases Mg_{5.05}Gd, Mg₂Gd, and Mg₃Gd will form due to non-equilibrium solidification during the casting process, and these second phases will disappear after hot-extrusion. The residual compressive stress exists in alloys after extrusion and increases with increasing Gd content. The existence of residual compressive stress contributes to the tensile strength. The elongation of all extruded alloys is over 30%, and the ultimate and yield tensile strength of the Mg–6Gd–0.6Zr alloy are 237 and 168 MPa, respectively. After isothermal aging for 10 h, the strength of extruded Mg–6Gd–0.6Zr alloys increases slightly, however, the elongation of alloys rarely decreases. The fracture mechanism of all studied alloys is ductile fracture.

Introduction

Rare earth magnesium alloys have been intensively studied for the past few decades due to their outstanding

mechanical properties at both room temperature and elevated temperature. Among them, the Mg–Gd alloys, which possess properties such as low density, excellent cast performance, superior mechanical properties, and good erosion resistance, have been the focus due to the needs in the automotive, architectural, and aerospace industries [1–4]. Previous investigations showed that magnesium alloys containing more than 10% (mass fraction) Gd demonstrated excellent mechanical properties at both room temperature and elevated temperature due to two major strengthening mechanisms: precipitation hardening and solid solution strengthening [5–16]. However, Gd can easily segregate in magnesium casting alloys, which makes the microstructure not uniform and decreases the mechanical properties, and the degree of segregation increases with increasing Gd content [15, 16]. Moreover, high Gd content can increase the alloy density and its cost, and decreases the ductility, limiting their commercial applications. Therefore, it is of great importance to study Mg–Gd alloys with low Gd content. The aim of this article is to investigate the microstructure and mechanical properties, as well as the strengthening mechanism of low Gd content magnesium alloys (with less than 10%Gd).

Experimental procedures

High purity Mg (99.8%, mass fraction), Mg–24.51%Gd, Mg–27.85%Zr master alloys were used as raw materials. The Mg– x Gd–0.6Zr ($x = 2, 4$, and 6%) alloys were synthesized by semi-continuous casting process. During melting, the master alloys were cleaned and preheated to 200–250 °C first; Mg was completely melted in well style electric resistance furnace at about 720 °C and cooled down to 680 °C; after that, the preheated Mg–24.51%Gd master alloy was

Y.-B. Hu (✉) · J. Deng · C. Zhao · F.-S. Pan · J. Peng
College of Materials Science and Engineering, Chongqing University, Chongqing 400044, China
e-mail: yaobohu@cqu.edu.cn

Y.-B. Hu · J. Deng · C. Zhao · F.-S. Pan · J. Peng
National Engineering Research Center for Magnesium Alloys,
Chongqing 400044, China

added into the Mg melt, and the temperature was increased to 720 °C again; after stirring for 2 min, preheated Mg–27.85%Zr master alloy was added and the temperature was increased to 760 °C; after stirring for 15 min the melt was placed for 3 min then cast into a thin-walled, water-cooled cylinder with 92 mm in diameter. Protection measures were taken during the whole process and CO₂/SF₆ gases were used during stirring and casting. Compositions of the as-cast alloys were determined by XRD-1800 CCDE X-ray fluorescence spectrometry, as shown in Table 1.

During extrusion, the as-cast GKx ($x = 2, 4$, and 6%) alloys were first preheated to 480 °C and held for 20 min, and then extruded at 450 °C with a extrusion ratio of 28 and a extrusion rate of 2.1 m/min. The resulting alloys are labeled as GKx-Ext ($x = 2, 4$, and 6%). GK6-Ext was heat treated with 200 °C/10 h (GK6-Ext-T5/10 h) and 200 °C/20 h (GK6-Ext-T5/20 h) to study the aging effect. Microstructures were analyzed by optical microscopy (OM, MDS produced by OPTEC Company), X-ray diffraction (XRD, D/max-1200, Cu, 40 kV/250 mA, 4°/min, 10–90°), and scanning electron microscope (SEM, VEGA II LMU). Micro-hardness tests were carried out under 50 g load and 10 s dwell time. The club-shaped specimens for tensile test were prepared according to the standard of GB/T 228-2002. The tensile test was conducted on XYB305C omnipotent tensile machine at a rate of 4 mm/min. The residual stress before and after surface treatment on GK6-Ext was studied by XRD method. In this study, $\sin^2\Psi$ (Ψ is X-ray incident angle, $\Psi = -45^\circ, -30^\circ, -15^\circ, 0^\circ, 15^\circ, 30^\circ$, and 45°) method was used to calculate the stresses. The parameters used in calculation were elasticity modulus 45 GPa, Poisson's ratio 0.35, diffraction angle range 111–116°, diffraction plane(300), method of determining peak position: half-width method, voltage 40 kV, and current 150 mA.

Results and discussion

The residual stress calculation

The $\sin^2\Psi$ method can be expressed by the following equations [17–20]:

Table 1 Nominal and actual composition of alloys

Code	Nominal composition (wt%)	Actual composition					
		wt%			at.%		
		Gd	Zr	Mg	Gd	Zr	Mg
GK2	Mg–2Gd–0.6Zr	1.681	0.333	Bal.	0.320	0.102	Bal.
GK4	Mg–4Gd–0.6Zr	3.845	0.480	Bal.	0.747	0.149	Bal.
GK6	Mg–6Gd–0.6Zr	6.501	0.380	Bal.	1.291	0.121	Bal.

$$\sigma_\varphi = -\frac{E}{2(1+v)} \times \frac{1}{\tan \theta_0} \times \frac{\prod}{180} \times \frac{\partial 2\theta}{\partial \sin^2 \psi} = KM$$

$$K = -\frac{E}{2(1+v)} \times \frac{1}{\tan \theta_0} \times \frac{\prod}{180}, M = \frac{\partial 2\theta}{\partial \sin^2 \psi}.$$

where σ_φ is the residual stress, positive value means tensile stress and negative value is compressive stress; E is the elasticity modulus; v is the Poisson's ratio; θ_0 is the diffraction half-angle when $\Psi = 0$; K is the stress constant; and M is the stress factor. This is a non-destructive method of measuring surface residual stress. The residual stress was calculated through strain, which can be determined by the change in the spacing of a certain plane. The strain ε_φ of spacing d is calculated by the equation as

$$\varepsilon_\varphi = \frac{d - d_0}{d_0} \%$$

It is known that the relationship between the spacing and diffraction half-angle theta can be conveyed by famous Bragg's equation as

$$2d\sin\theta = \lambda$$

where λ is wavelength of incident ray.

The residual stress calculation was done by Jade 6.0 software. Compared with the professional residual stress instruments, the results are not very accurate, but it can show the type and evolution trend of the residual stresses.

The effect of Gd on microstructure and mechanical properties of as-cast GKx alloys

The microstructures of the as-cast GKx ($x = 2, 4$, and 6%) alloys are typical grain structures and no Gd dendritic segregation (as shown in Fig. 1). The constitutional supercooling and the temperature gradient in liquid before the liquid–solid interface are the two major factors determining the microstructure of the as-cast alloy. In general, it is easy to form dendritic microstructure due to the negative temperature gradient and the existence of the second impurity atoms during casting. It has also been reported [15, 16] that it is easy for Gd to segregate in magnesium casting alloys, making the microstructure not uniform and decreasing the properties. The particles formed by segregation of rare earth elements can pile-up dislocations, impede the motion of grain boundary, and become the sites of crack initiation, resulting in low plasticity and exerting influence on fracture mechanism. From Fig. 1, it can be concluded that low Gd contents, combining with proper casting conditions, can result in positive temperature gradient in liquid before the liquid–solid interface.

The mean grain size was measured by linear intercept method. The grain size of the as-cast GKx ($x = 2, 4$, and 6%) alloys is 41, 27, and 55 μm, respectively. The Zr contents in GK4 alloy are slightly higher than other two alloys, shown in Table 1. There is no strong correlation

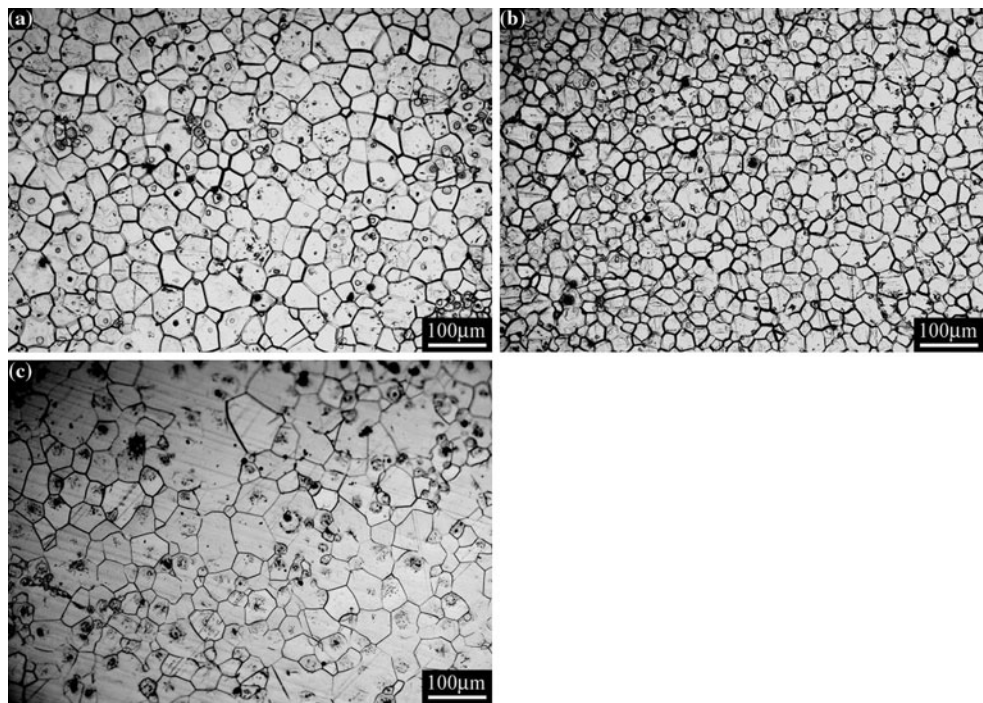


Fig. 1 Optical micrographs of as-cast GK x ($x = 2, 4$, and 6%) alloys. **a** GK2, **b** GK4, and **c** GK6

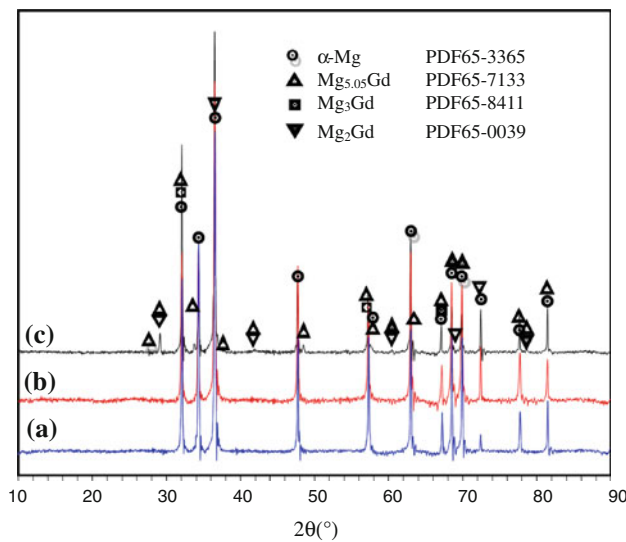


Fig. 2 XRD results of as-cast GK x ($x = 2, 4$, and 6%) alloys. **(a)** GK2, **(b)** GK4, and **(c)** GK6

between grain size and Gd content because this is due to the addition of Zr, which can refine the grain size. Moreover, the addition of Zr will not cause new phase precipitate out from the Mg–Gd alloys [21].

Figure 2 shows the XRD results of the as-cast GK x ($x = 2, 4$, and 6%) alloys. No second phase but the α -Mg solid solution appears in GK2 and GK4 alloys. However, as Gd content increases, new phase appears. In

Table 2 Crystal lattice parameters of magnesium and α -Mg solid solution of GK x , GK x -Ext ($x = 2, 4$, and 6%), GK6-Ext-T5/10 h, and GK6-Ext-T5/20 h alloys

Alloys	a (Å)	c (Å)
Mg	3.20890	5.21010
GK2	3.21213	5.21369
GK4	3.21405	5.21441
GK6	3.21726	5.21256
GK2-Ext	3.21818	5.22045
GK4-Ext	3.21528	5.21728
GK6-Ext	3.21266	5.21638
GK6-Ext-T5/10 h	3.21675	5.21847
GK6-Ext-T5/20 h	3.21666	5.21853

GK6 alloy, Mg_{5.05}Gd, Mg₃Gd, Mg₂Gd, and α -Mg solid solution are detected (Fig. 2). From the Mg–Gd phase diagram, it is known that the equilibrium second phases Mg_xGd ($x \leq 3$) appear when Gd contents are over 53 wt%. Therefore, the appearance of Mg₂Gd and Mg₃Gd phases is due to the non-equilibrium solidification during the casting process.

The crystal lattice parameters of α -Mg solid solution in the as-cast GK x ($x = 2, 4$, and 6%) alloys were calculated by Jade 5.0 software (shown in Table 2). The crystal lattice parameters a and c of α -Mg solid solution are larger in three alloys than those in Mg, which should be the result that some second impurity atoms are dissolved into the

matrix. For GK2, GK4 alloys, almost all of Gd was dissolved into the matrix. As for GK6, some Gd was dissolved into the matrix and some precipitated with Mg, which is shown in the XRD patterns (Fig. 2).

Figure 3 shows the 25-site micro-hardness test results of the as-cast GK_x ($x = 2, 4$, and 6%) alloys, the black squares are the average value of each group. The distribution of micro-hardness is relatively centralized, which indicates that the uniformity of alloys is good. It can be seen from Fig. 3 that the hardness value increases with increase in Gd content, and dHV/dx ($x = 4\text{--}6\%$) is higher than dHV/dx ($x = 2\text{--}4\%$).

Grain refinement, precipitation hardening, and solid solution strengthening are some major strengthening mechanisms for magnesium alloys. The hardness of GK4 alloy is higher than that of GK2 alloy; this can be explained in two aspects. First, Gd is completely dissolved into the matrix in both alloys and GK4 has higher Gd content than GK2 (shown in Fig. 2 and Table 2). Second, the grain size of GK4 is smaller (Fig. 1a, b). So both solid solution strengthening and grain refinement are contributive to the increase in micro-hardness of as-cast GK4 alloy. With the further increase of Gd content, the second phase appears, which can further improve the strength and make the hardness per unit Gd content obviously increased, in other word, dHV/dx ($x = 4\text{--}6\%$) is higher than dHV/dx ($x = 2\text{--}4\%$).

The effect of Gd on microstructure and mechanical properties of GK_x -Ext alloys

Compared with the microstructure of the as-cast GK_x ($x = 2, 4$, and 6%) alloys (as shown in Fig. 1), the grain sizes of all the GK_x ($x = 2, 4$, and 6%)-Ext alloys are

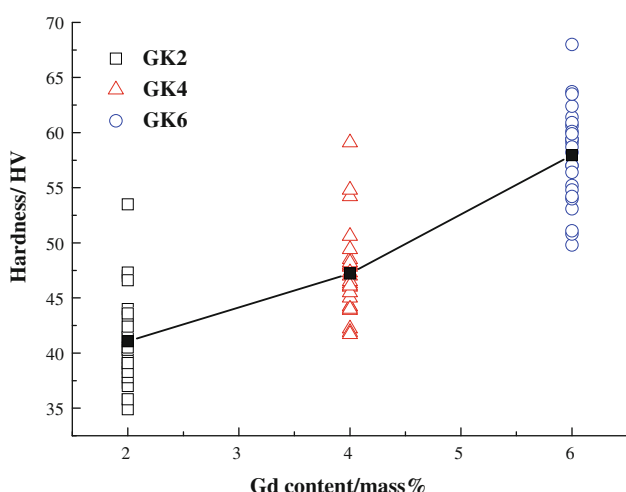


Fig. 3 Micro-hardness results of as-cast GK_x ($x = 2, 4$, and 6%) alloys

greatly refined and become comparatively consistent, about $10\ \mu\text{m}$ (as shown in Fig. 4). Hot-extrusion is one of the most effective ways in microstructure refinement. In extrusion process, initial grains were destroyed and dispersed, and dynamic recrystallization occurred. Initial grains hold back the growth of recrystallized grains, which results in microstructure refinement. It can be seen that the recrystallization extents are different in three alloys, slightly weaker in GK2 alloy (Fig. 4a).

Figure 5 shows the XRD results of GK_x ($x = 2, 4$, and 6%)-Ext alloys. It can be seen that there is no other second phase except $\alpha\text{-Mg}$ solid solution. The second phases $Mg_{5.05}\text{Gd}$, $Mg_3\text{Gd}$, and $Mg_2\text{Gd}$ in GK6 disappeared after extrusion. From the peak shifting of XRD results of GK_x ($x = 2, 4$, and 6%)-Ext alloys (shown in Fig. 6), it can be seen that with the increasing of Gd content, the peak shifts to higher angles, values of lattice parameters decreases, which is shown in Table 2.

The volume of second phase in alloys is small. During extrusion, the second phase is broken up and distributed uniformly. Parts of these broken and fine second phases are dissolved into the matrix by diffusion and/or other means due to the high temperature at extrusion. As a result, the crystal plane spacing will increase and crystal lattice parameters and c also will increase. Nevertheless, the residual stress accumulated from extrusion cannot be released immediately. The residual tensile stress makes the crystal plane spacing and lattice parameter of $\alpha\text{-Mg}$ solid solution increase. The residual compressive stress, on the contrary, will cause decrease in the crystal plane spacing and lattice parameter. From the peak shifting results (as shown in Fig. 6), with the increasing of Gd content, the crystal lattice parameters are supposed to increase, but due to the effect of residual compressive stress, the values of a and c all decrease (as shown in Table 2). In other word, the addition of Gd causes residual compressive stress increase in extrusion, and the more Gd content, the higher amount of residual compressive stress.

Table 3 shows the ultimate tensile strength, yielding tensile strength and elongation of the alloys studied. The strength of GK2-Ext and GK4-Ext is about the same, 207 and 206 MPa, respectively for the ultimate tensile strength, 150 and 145 MPa, respectively for the yield tensile strength. The ultimate tensile strength and the yield tensile strength of GK6-Ext are the highest among the three alloys, 237 and 168 MPa, respectively. The elongation of GK4-Ext is the highest, reaching 43.35%, which means there is a most suitable Gd content for elongation.

The grains of GK_x ($x = 2, 4$, and 6%)-Ext alloys are refined to about $10\ \mu\text{m}$ (as shown in Fig. 4). Therefore, the difference of stress inside the grain and around boundary is small. As a result, alloys will not fracture due to stress concentration and can subject to large deformation before

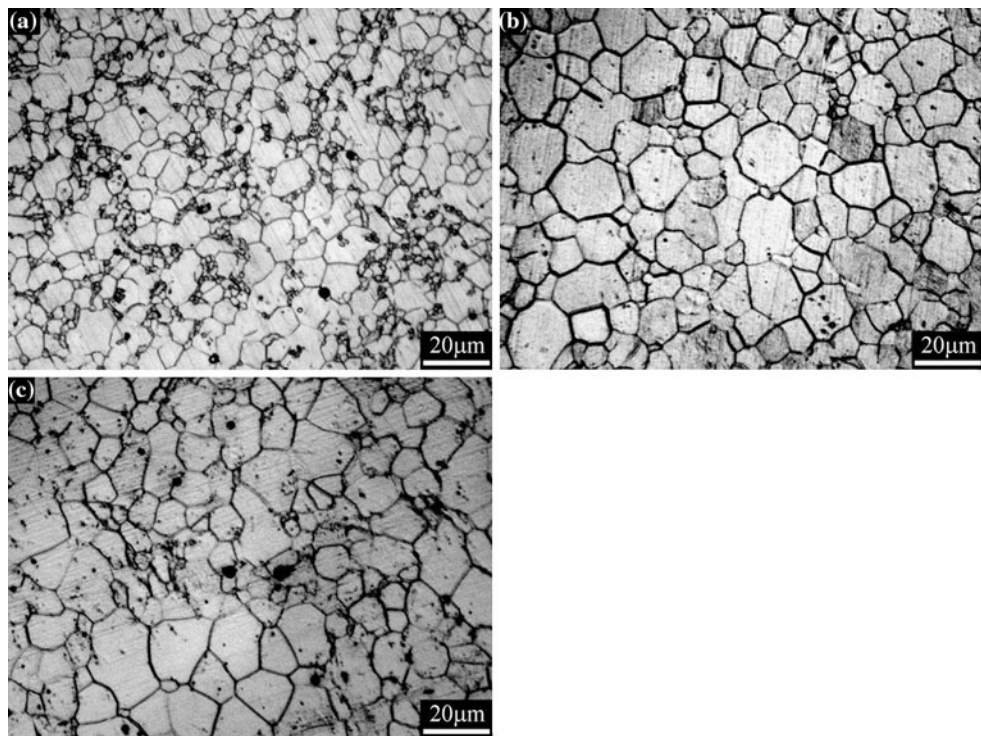


Fig. 4 Optical micrographs of GK_x ($x = 2, 4$, and 6%)-Ext alloys. **a** GK2, **b** GK4, and **c** GK6

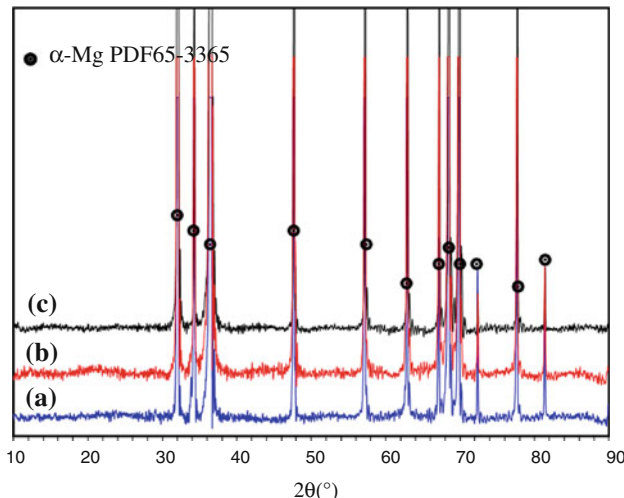


Fig. 5 XRD patterns of GK_x ($x = 2, 4$, and 6%)-Ext alloys. **(a)** GK2, **(b)** GK4, and **(c)** GK6

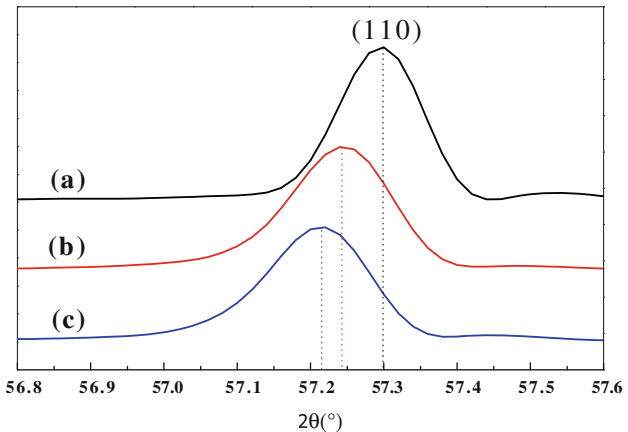


Fig. 6 Peak shifting of XRD pattern of GK_x ($x = 2, 4$, and 6%)-Ext alloys due to Gd addition. **(a)** GK2, **(b)** GK4, and **(c)** GK6

fractured, making these alloys have high elongation prior to fracture. Figure 7 shows a large of parallel dislocations direction in GK4-Ext alloy. The decreases of c/a and yield phenomenon can all contribute to the plasticity of alloys [22]. The micro-mechanism of plasticity of these alloys will be reported elsewhere. With the increasing of Gd content, more Gd is dissolved into the matrix, i.e., the strength will be higher due to solid solution strengthening. Moreover, higher Gd content will cause higher residual

Table 3 Mechanical properties of Mg–Gd–Zr alloys

Alloys	UTS (MPa)	YTS (MPa)	El. (%)
GK2-Ext	207	150	36.8
GK4-Ext	206	145	43.4
GK6-Ext	237	168	33.4
GK6-Ext-T5/10 h	243	179	31.7
GK6-Ext-T5/20 h	220	153	32.3

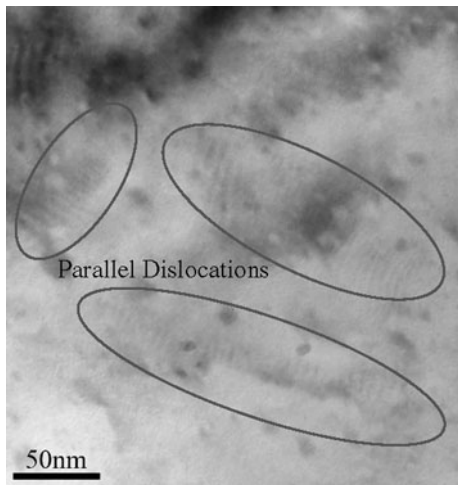


Fig. 7 Dislocations direction in GK4-Ext alloys

compressive stress. This residual stress can improve the strength of alloys to some extent. Thus, the strength of GK4-Ext should be higher than that of GK2-Ext. However, from Table 3, the ultimate tensile strength of GK2-Ext and GK4-Ext is close. This can be explained by the fact that residual stress can bring in lattice defects such as dislocation. Consequently, the density of the dislocation increases. When alloys are subjected to external force, the movable dislocation will move. Once plenty of dislocations reach the boundary, the boundary has a high chance to move, which can decrease then the strength. Therefore, more Gd can both increase and decrease the strength and as a result, there is no much difference between GK2-Ext and GK4-Ext in ultimate tensile strength. For GK6-Ext, the strength is improved by the solid solution strengthening and residual compressive stress. This time, the residual compressive stress is plenty enough to make the density dislocation multiple. The plenty of dense dislocation twists to baffle dislocation to move further. In the other words, the density of dislocations increases, but movable dislocation decreases. So the strength of GK6-Ext increases due to the combination of solid solution strengthening, residual compressive stress, and the decrease of movable dislocation density.

The effect of aging time on microstructure and mechanical properties of GK6-Ext alloys

Figure 8 shows the SEM results of as-cast, aged 10 h, and aged 20 h GK6-Ext alloys. The size of the big grain of GK6-Ext alloy is about 10 μm , surrounded by some small grains formed in extrusion. Strip-like “hollow” phases can be seen within the white area inside some large grains; while some round “hollow” phases surrounded by white area can be seen at the grain boundaries. With the increase

of aging time, the grain size does not change, but the white area inside grain enlarges, some strip-like “hollow” phases become round “hollow” phases and some “hollow” phases at the grain boundaries grow up. Some white dot-like phases, which are about 1 μm in size, precipitate beside the “hollow” phases at the grain boundaries.

With the increase in aging time, $\text{Mg}_{5.05}\text{Gd}$ phase deposits (as shown in Fig. 9) and the a/c of $\alpha\text{-Mg}$ in GK6-Ext-T5/10 h and GK6-Ext-T5/20 h are increased. Aging makes the dissolved second atom deposit, which reduces both the spacing of crystal planes and the values of lattice parameters. However, the residual compressive stress is released during aging, which makes the spacing and a/c increase. Crystal lattice parameters a/c of GK6-Ext-T5/10 h are increased (shown as in Table 2), which means the effect of residual stress release dominates. There is no much difference between GK6-Ext-T5/10 h and GK6-Ext-T5/20 h (as shown in Table 3). This is because after aging for 20 h, more $\text{Mg}_{5.05}\text{Gd}$ phases deposit from $\alpha\text{-Mg}$ solid solution, but at the same time, residual compressive stress is further released. The effect due to the residual compressive stress release offsets that due to second phase’s deposition, and as a result, the change of a/c is small.

With the increase in aging time, the strength also increases, but after aged for 20 h, the strength decreases. Surprisingly, the elongation is almost same after different aging time (Table 3). As previous analysis, the residual compressive stress can improve the tensile strength of alloys. So after aged 10 h, part of the residual compressive stress is released, thus the strength decreases. However, the second phase deposition can improve the strength. The combination of these two effects will determine the strength of the alloys. If the effect of second phase deposition dominates, the ultimate tensile strength and yield tensile strength will increase. To further prove the type of residual stress and find out the change of residual stress between GK6-Ext and GK6-Ext-T5/10 h alloys, the residual stress calculation was made and the results are shown in Fig. 10.

After aging for 20 h, the residual compressive stress is completely released, which makes the strength decrease obviously. Although more second phase can deposit with long aging time, the total amount of second phases is limited, which cannot offset the decrease of the strength due to residual stress release. As a result, the strength decreases after aging for 20 h. The suitable aging time for strengthening GK6-Ext alloy is 10 h. As the grain size is scarcely changed (as shown in Fig. 8) during aging, the alloys have retained excellent plasticity. Consequently, GK6-Ext-T5/10 h alloy possesses both receivable strength and excellent plasticity.

From the view of macro-plasticity and the fracture surface feature, the fracture mechanism of GK6-Ext-T5/20 h alloy

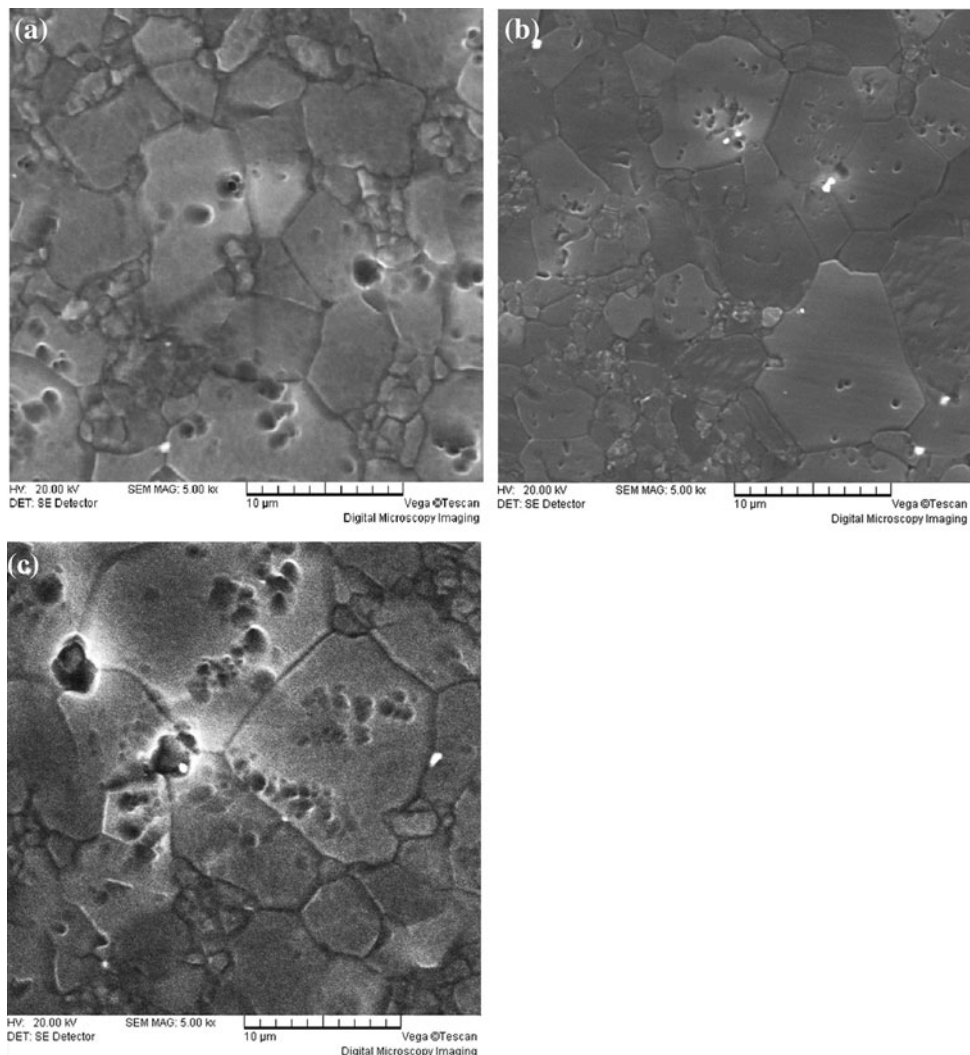


Fig. 8 SEM results of GK6 alloys. **a** GK6-Ext; **b** GK6-Ext-T5/10 h; and **c** GK6-Ext-T5/20 h

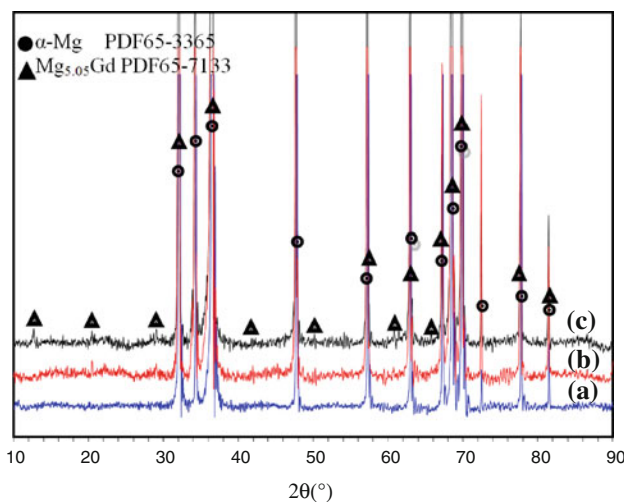


Fig. 9 XRD results of GK6 alloys. **(a)** GK6-Ext; **(b)** GK6-Ext-T5/10 h; and **(c)** GK6-Ext-T5/20 h

should be ductile fracture. Figure 11 shows the SEM results of the tensile fracture surface of GK6-Ext-T5/20 h alloy. Some white dots can be seen in the ductile nest (Fig. 11b). The small white dots are the focuses of the stress concentration when the alloy is being loaded. The matrix around white dots forms micro hollows at the concentrated stress, and the micro hollows become big and start interconnecting each other. When big hollows continue to grow up and connect mutually, alloy will fracture.

Conclusions

1. The as-cast Mg– x Gd–0.6Zr ($x = 2, 4$, and 6%) alloys have grain structure without Gd segregation in the microstructure. In Mg–6Gd–0.6Zr alloy, the second phase Mg_{5.05}Gd, Mg₂Gd, and Mg₃Gd were formed due to non-equilibrium solidification during the casting

Fig. 10 Residual stress of **a** GK6-Ext and **b** GK6-Ext-T5/10 h

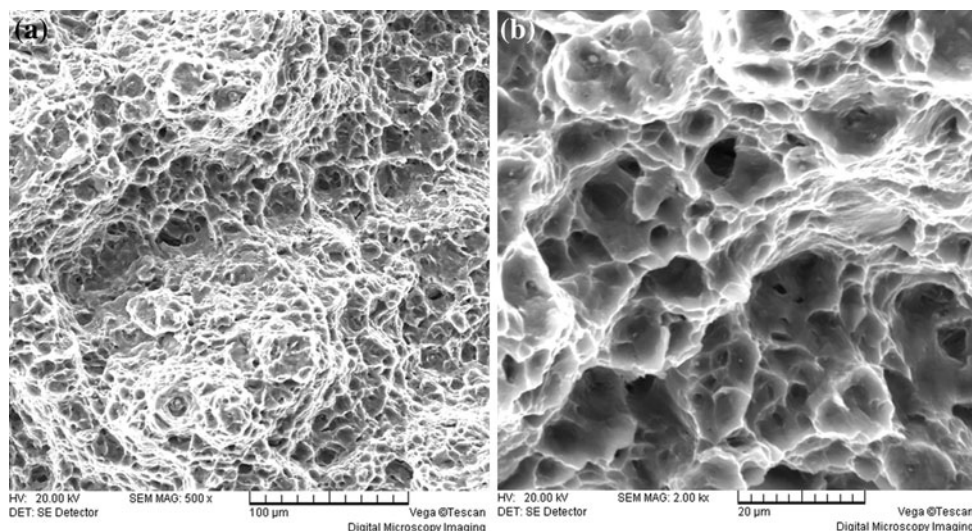
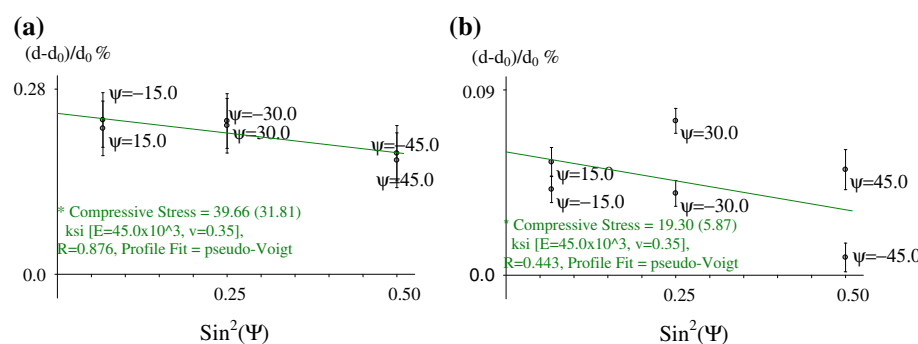


Fig. 11 Fractographs of GK6-Ext-T5/20 h alloy. **a** low magnification of GK6 fracture surface. **b** high magnification of GK6 fracture surface

- process. These second phases will disappear after extrusion. With the increasing of Gd content, the second phase appears, which can further improve the strength and increase the hardness per unit Gd content and dHV/dx ($x = 4\text{--}6\%$) is bigger than dHV/dx ($x = 2\text{--}4\%$).
 2. The residual compressive stress in alloys after extrusion increases with increasing Gd content. The existence of residual compressive stress is contributive to the tensile strength of alloys. The elongation of all extruded alloys is over 30%, and the ultimate and yield tensile strength of Mg–6Gd–0.6Zr alloy are 237 and 168 MPa, respectively.
 3. After aged for 10 h, the strength of extruded Mg–6Gd–0.6Zr alloy increases slightly, at the same time, elongation of alloys rarely decreases. The fracture mechanism of this alloy is ductile fracture.

Acknowledgements This study is supported by the Fundamental Research Funds for the Central Universities (Project no. CDJZR10130020).

References

- Yang MB, Cheng L, Pan FS (2009) J Mater Sci 44:4577. doi: 10.1007/s10853-009-3693-0
- Shigeharu K, Shigeru I, Kyoaki O (1992) Jpn J Inst Light Met 42(12):727
- Shigero I, Yuji N, Shigeharu K (1994) Jpn J Inst Light Met 144(1):1
- Li DJ, Wang QD, Blandin JJ (2009) Mater Sci Eng A 526(1/2):150
- Peng QM, Wu YM, Fang DQ, Meng J, Wang LM (2007) J Alloy Compd 430:252
- Peng QM, Hou XL, Wang LD, Wu YM, Cao ZY, Wang LM (2009) Mater Design 30:292
- Wang R, Dong J, Fan LK, Zhang P, Ding WJ (2008) Trans Nonferrous Met Soc China 18:189
- Zheng KY, Dong J, Zeng XQ, Ding WJ (2008) Mater Charact 59:857
- Anyanwu IA, Kamado SY (2001) Mater Trans 42:1206
- Kawabata T, Matsuda K, Kamado S (2003) Mater Sci Forum 419–422:303
- Liu K, Zhang JH, Rokhlin LL, Elkin FM, Tang DX, Meng J (2009) Mater Sci Eng A 505:13
- Balasubramani N, Pillai UTS, Pai BC (2008) J Alloys Compds 460:6

13. Liu K, Zhang JH, Su GH, Tang DX, Rokhlin LL, Elkin FM, Meng J (2009) *J Alloys Compd* 481:811
14. Xiao Y, Zhang XM, Chen BX, Deng ZZ (2006) *Trans Nonferrous Met Soc China* 16:1669
15. Peng QM, Dong HW, Wang LD, Wu YM, Wang LM (2008) *Mater Sci Eng A* 477:193
16. Yang Z, Li JP, Gao YC, Liu T, Xia F, Zeng ZW, Liang MX (2007) *Mater Sci Eng A* 454:274
17. Yuan FR, Wu SL (1987) Measurement and calculation of residual stress. Hunan University Press, Changsha
18. Zhang DQ, He JW (1999) Residual stress analysis by X-ray diffraction and its function. Xi'an Jiaotong University Press, Xi'an
19. Jankowski AF, Saw CK, Ferreira JL, Harper JS, Hayes JP, Pint BA (2007) *J Mater Sci* 42:5722. doi:[10.1007/s10853-006-0658-7](https://doi.org/10.1007/s10853-006-0658-7)
20. Gautam A, Tripathy P, Raw S (2006) *J Mater Sci* 41:3007. doi:[10.1007/s10853-006-6768-4](https://doi.org/10.1007/s10853-006-6768-4)
21. Sun M, Wu GH, Wang W, Ding WJ (2009) *Mater Sci Eng A* 523:145
22. Agnew SR, Yoo MH, Tome CN (2001) *Acta Mater* 49(20):4277